



Discovery and SAR of spirochromane Akt inhibitors

Nicholas C. Kallan^{a,*}, Keith L. Spencer^a, James F. Blake^a, Rui Xu^a, Justin Heizer^a, Josef R. Bencsik^a, Ian S. Mitchell^a, Susan L. Gloor^a, Matthew Martinson^a, Tyler Risom^a, Stefan D. Gross^a, Tony H. Morales^a, Wen-I Wu^a, Guy P. A. Vigers^a, Barbara J. Brandhuber^a, Nicholas J. Skelton^b

^a Array BioPharma, Inc., 3200 Walnut Street, Boulder, CO 80301, USA

^b Genentech, Inc., 1 DNA Way, South San Francisco, CA 94080-4990, USA

ARTICLE INFO

Article history:

Received 17 December 2010

Revised 15 February 2011

Accepted 16 February 2011

Available online 18 February 2011

Keyword:

Akt kinase inhibitors

ABSTRACT

A novel series of spirochromane pan-Akt inhibitors is reported. SAR optimization furnished compounds with improved enzyme potencies and excellent selectivity over the related AGC kinase PKA. Attempted replacement of the phenol hinge binder provided compounds with excellent Akt enzyme and cell activities but greatly diminished selectivity over PKA.

© 2011 Elsevier Ltd. All rights reserved.

Akt, also known as protein kinase B (PKB), is an intracellular anti-apoptotic serine/threonine kinase in the AGC kinase family, and it is comprised of three isoforms: Akt1, Akt2, and Akt3. These isoforms have ca. 90% sequence identity in the kinase domain and 97–100% sequence identity in the ATP-binding site.¹ The PI3K/Akt pathway is a major signaling axis for cell growth, proliferation, and apoptosis, and it is upregulated in many cancers.² Aberrant Akt signaling can occur via a number of mechanisms, including oncogenic PI3K mutations, loss of PTEN tumor suppressor function, Akt over-expression, and therapeutic-induced pathway activation. Owing to these factors, significant interest exists in finding inhibitors of components of this pathway for cancer treatment.³

A high throughput screening (HTS) campaign identified compounds **1** and **2** as low μM hits (Fig. 1).⁴ Interestingly, further profiling of compound **1** showed that it displayed selectivity (>25-fold) versus the closely related AGC family kinase protein kinase A (PKA). Achieving general kinase selectivity, especially for Akt over PKA, is known to be both important and challenging.⁵ This became a key driver for further exploring structure–activity relationships (SAR) in this class of compounds.

Based on HTS hits **1** and **2**, an initial set of analogs was prepared as shown in Scheme 1. Substituted sulfonyl chlorides were reacted with a variety of primary amines to give the corresponding sulfonamides **3**, which were then deprotonated with NaH and treated with (*R*)-epichlorohydrin to generate epoxides **4**. The racemic spirochromane core was prepared by condensing 2′/5′-dihydroxyacetophenone with 1-Boc-3-piperidone to afford Boc intermediate **5**. Boc removal with HCl/dioxane, followed by

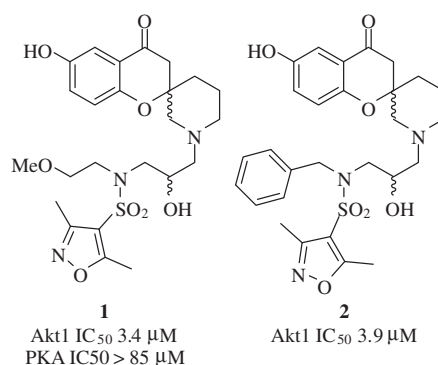


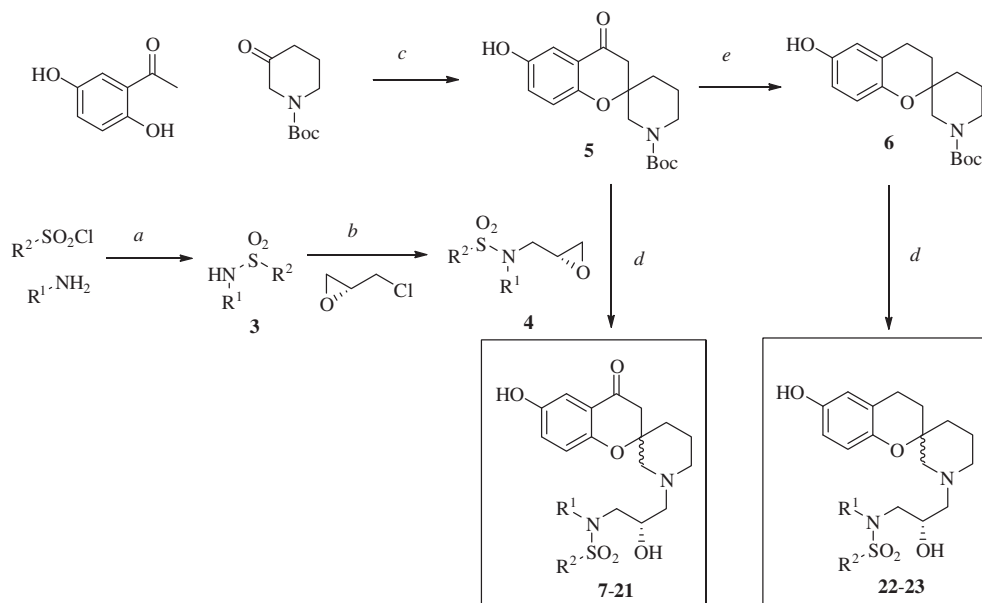
Figure 1. HTS hits **1** and **2**.

treatment with **4** furnished spirochromanes **7–21** as 1:1 mixtures of diastereomers at the spiropiperidine stereocenter. In addition, a set of des-keto spirochromane analogs was also prepared. The ketone in **5** was reduced with NaBH₄ to give the corresponding benzylic alcohol, which was removed by hydrogenolysis with Pd/C under an atmosphere of hydrogen to provide **6**. Boc deprotection with HCl/dioxane, followed by treatment with **4**, furnished analogs **22** and **23** as 1:1 mixtures of diastereomers at the spiropiperidine stereocenter.

Compounds **7–23** (Tables 1 and 2) were evaluated in vitro for inhibition of Akt1⁶ and in LNCaP cells for formation of phosphorylated PRAS40.⁷ A modest potency difference was observed between secondary hydroxyl diastereomers (Table 1, compare **7**, prepared

* Corresponding author.

E-mail address: nkallan@arraybiopharma.com (N.C. Kallan).



Scheme 1. Reagents and conditions: (a) TEA, DCM; (b) NaH, DMF; (c) pyrrolidine, MeOH, 50 °C; (d) (i) HCl/dioxane; (ii) **4**, TEA, EtOH, 60 °C; (e) (i) NaBH₄, MeOH; (ii) Pd/C, 1 atm H₂, EtOH.

from (*R*)-epichlorohydrin, and **8**, prepared from (*S*)-epichlorohydrin); thus all further analogs were prepared using (*R*)-epichlorohydrin. The spiro-piperidine diastereomers of compound **7** were also separated via preparative HPLC (**7-d1** and **7-d2**), and a 20-fold difference in potency was observed between them.⁸ For simplicity, the rest of the compounds were assayed as 1:1 mixtures of diastereomers at the spiro-piperidine stereocenter. We also found that removal of the secondary alcohol resulted in >30-fold loss in potency (data not shown).

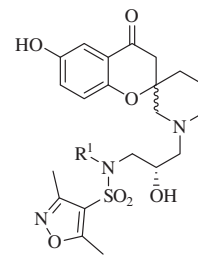
For the amine side chain R¹, the best substituents were small alkyl ethers (Table 1). Ethoxyethyl analog **9** (1.0 μM) and isopropoxyethyl derivative **10** (0.3 μM) showed improved potencies relative to methoxymethyl compound **7** (6.5 μM), while larger ether substituents lost potency (data not shown). Alkyl groups gave similar potencies to the corresponding ethers (e.g., **9** vs **11**), but the ether derivatives were preferred due to their lower ClogP values. Cycloalkyl substituents were also examined and lost potency relative to the ethers (cf. **12**). In addition, benzyl derivatives were explored and showed modest potencies, but these were not investigated further in order to keep both MW and ClogP low (data not shown). Ultimately, the ethoxyethyl side chain provided the optimum balance between potency, size, and ClogP, and this amine substitution was preserved as we probed sulfonamide SAR.

Modeling suggested that the sulfonamide group would bind in the somewhat narrow hydrophobic P-loop region of Akt, and in general, we found that aromatic and heteroaromatic rings substituted with small lipophilic groups were best. While the *meta*- and *para*-chlorophenyl derivatives **13** and **14** were inactive (≥20 μM), the Akt1 potency of the *ortho*-chlorophenyl analog **15** was 1.0 μM (Table 2). Although larger groups were not tolerated (data not shown), further exploration at the *ortho* position produced sub-micromolar analogs, including the 2,6-dimethyl derivative **21** (0.3 μM against Akt1). Benzyl and larger bicyclic aromatic ring systems all lost potency relative to the substituted monocycles, and removal of the arylsulfonyl group completely abolished activity (data not shown). Turning to the spirochromanone core, removal of the ketone resulted in further improvement in enzyme potency (e.g., **9** vs **22**). Thus, combining 2,6-dimethyl phenyl substitution with ketone removal provided the most potent analog to this point (**23**). Gratifyingly, the PKA selectivity of the initial

HTS lead **1** was preserved in all of the optimized analogs. All compounds in Tables 1 and 2 had a PKA enzyme IC₅₀ >10 μM, with compound **23** showing >250-fold selectivity.

The more potent phenol-based analogs in Table 2 achieved excellent PKA selectivity and reasonable enzyme potency, but none attained cell potency below 2.6 μM observed for **23**. Analysis of several X-ray crystal structures of phenol-based analogs bound to Akt1 indicated that the phenol OH forms less than optimal hydrogen bonding interactions with the hinge residues (Glu228 and Ala230) due to relatively elongated acceptor–donor distances (cf., Fig. 2, compound **21**). The phenol O is located 3.5 Å from the nitrogen of Ala230 and 3.9 Å from the backbone carbonyl oxygen of Glu228. Phenol replacements were thus explored in an attempt

Table 1
Amine side chain SAR



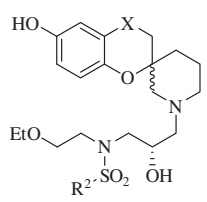
Compd	R ¹	Akt1 IC ₅₀ ^a (μM)	pPRAS40 IC ₅₀ ^b (μM)
7	CH ₂ CH ₂ OMe	6.5	>25
7-d1	CH ₂ CH ₂ OMe	2.1	>25
7-d2	CH ₂ CH ₂ OMe	40	>25
8^c	CH ₂ CH ₂ OMe	22.8	>25
9	CH ₂ CH ₂ OEt	1.0	>25
10	CH ₂ CH ₂ OiPr	0.3	18.6
11	CH ₂ (CH ₂) ₃ CH ₃	1.1	>25
12	Cyclohexyl	4.0	>25

^a Data is an average of three determinations.

^b Data is an average of two determinations.

^c (*S*)-Epichlorohydrin was used in Scheme 1, Step b.

Table 2
Sulfonamide and core modifications



Compd	R ²	X	Akt1 IC ₅₀ ^a (μM)	pPRAS40 IC ₅₀ ^b (μM)
13		C=O	>20	>25
14		C=O	~20	>25
15		C=O	1.0	>25
16		C=O	>20	>25
17		C=O	6.2	>25
18		C=O	4.4	>25
19		C=O	1.3	>25
20		C=O	0.5	>25
21		C=O	0.3	17.8
22		CH ₂	0.07	6.4
23		CH ₂	0.04	2.6

^a Data is an average of three determinations.

^b Data is an average of two determinations.

to improve potency and to remove the potential metabolic liabilities of this moiety.

Unsubstituted and fluoro-spirochromane intermediates **24** and **25** were prepared using 2'-hydroxyacetophenone and 5'-fluoro-2'-hydroxyacetophenone, respectively (Scheme 2). The Boc group in **25** was removed, followed by treatment with epoxide **26**⁹ to furnish fluoro analog **27**. A nitrile phenol replacement was synthesized in a similar manner. Bromination of intermediate **24** with NBS, followed by lithiation of the resulting bromide with tBuLi and subsequent treatment with tosyl cyanide afforded nitrile intermediate **28**. Boc removal with HCl/dioxane, followed by reaction with epoxide **26** gave **29**. Nitrile **28** was also converted to the primary amide by treatment with TFA/H₂SO₄ and subsequent reaction with epoxide **26** to afford **30**.

Other phenol replacements were investigated, such as constraining primary amide **30** into a lactam ring (Scheme 3). Thus,

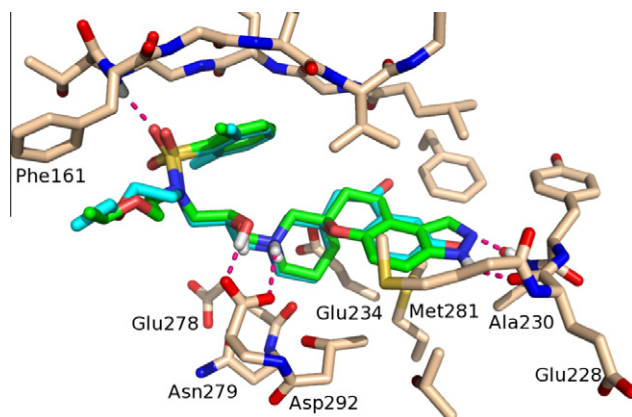


Figure 2. X-ray structure overlays of **21** (cyan) and **38** (green) bound to Akt1 (PDB accession codes 3QKK and 3QKL, respectively). Residue Lys179 was removed for clarity.

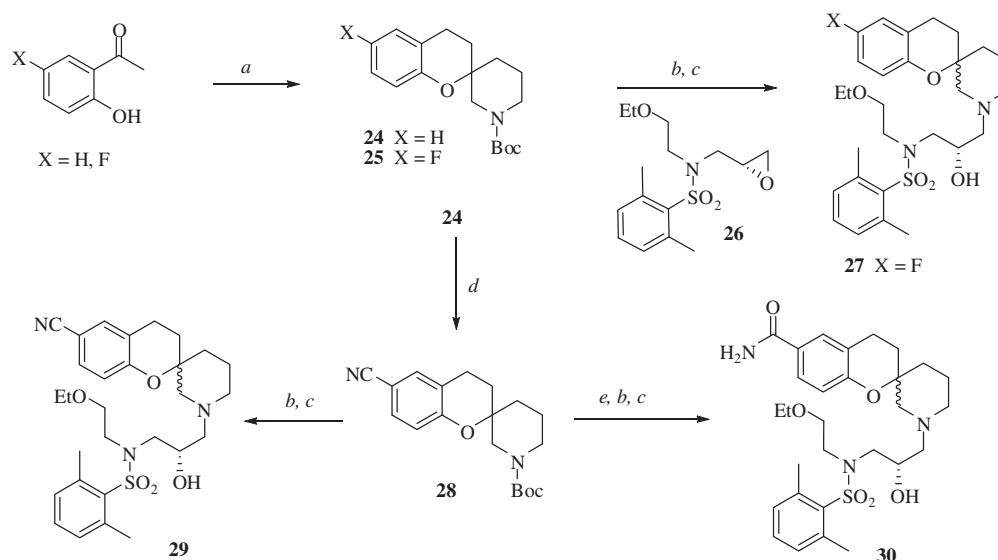
4'-cyano-2'-hydroxyacetophenone was first converted to spirochromane intermediate **31**.¹⁰ Nitrile reduction with NaBH₄/CoCl₂, followed by amine protection gave trifluoroacetamide **32**. Iodination with I₂/HIO₃, followed by deprotection furnished amine **33**. Intramolecular lactam formation was effected using a Pd-catalyzed carbonylation to give **34**, which after Boc removal and reaction with epoxide **26** provided lactam **35**.

In addition to phenol replacements, indazole was explored as a surrogate (Scheme 4). Diazotization of 4-methoxy-2-methylaniline, followed by indazole formation gave **36**. Friedel–Crafts acylation (with concomitant phenol deprotection) and subsequent condensation with Boc-3-piperidone furnished pyrazolo-spirochromane **37**. Finally, ketone removal followed by Boc deprotection and reaction with epoxide **26** provided **38**.

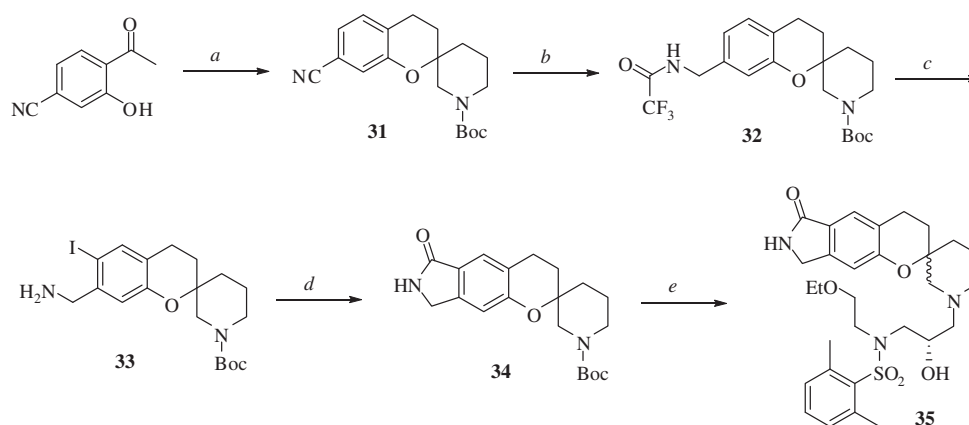
The potencies of the phenol replacements are shown in Table 3. Fluoro and nitrile analogs **27** and **29** exhibited only a slight reduction in Akt1 enzyme potency compared to phenol **23**, although PKA selectivity diminished somewhat to 50-fold. Interestingly, primary amide **30** showed improved Akt1 enzyme potency while retaining PKA selectivity (>385-fold), though its cell potency was still modest. However, in contrast to amide **30**, constraining the amide into a lactam (**35**) greatly improved cell potency, but unfortunately the PKA selectivity eroded to 5-fold. In addition, indazole **38** showed excellent enzyme and cell potencies, but again the PKA selectivity diminished to 3-fold.

In addition to X-ray crystal structures of the phenol-based series of inhibitors (e.g., **21**), we obtained a structure of **38** bound to Akt1 (Fig. 2). The secondary hydroxyls and protonated piperidine nitrogens of both compounds interact with the side chain carboxylate of Asp292. The secondary hydroxyls also interact with the catalytic Lys179. The 2,6-dimethyl phenyl groups pack underneath the hydrophobic P-loop, and the ethoxyethyl side chains form lipophilic contacts with the exposed side chain of Phe161 at the tip of this loop, in addition to a hydrogen bond that is formed between the backbone NH and one of the sulfonamide oxygens.

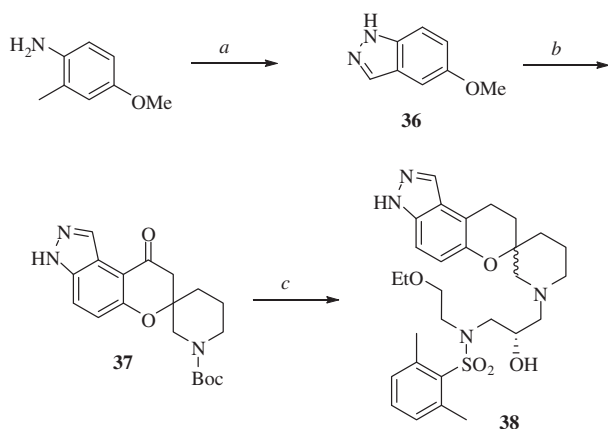
The data presented above highlight a distinct difference between inhibition of Akt1 and PKA, in that inhibition of Akt1 is not greatly affected by hinge contacts (e.g., 4-fold potency difference between phenol **23** and indazole **38**), whereas PKA is greatly affected (>330-fold potency difference between **23** and **38**). Examination of Figure 2 shows that all of the other components in both phenol **21** and indazole **38** — the spiro-piperidines, secondary alcohols, sulfonamides, and amine side chains — overlay almost exactly, and the only differences lie in the hinge region. For indazole **38** bound to Akt1, the indazole NH to Glu228 carbonyl



Scheme 2. Reagents and conditions: (a) (i) Boc-3-piperidone, pyrrolidine, MeOH, 50 °C; (ii) NaBH₄, MeOH; (iii) Pd/C, 1 atm H₂, EtOH; (b) HCl/dioxane; (c) **26**, TEA, EtOH, 60 °C; (d) (i) NBS, 10 mol % 1 M HCl, acetone; (ii) tBuLi, THF, -78 °C; TsCN; (e) TFA, H₂SO₄; then Boc₂O, dioxane.



Scheme 3. Reagents and conditions: (a) (i) Boc-3-piperidone, pyrrolidine, MeOH, 50 °C; (ii) NaBH₄, MeOH; (iii) Et₃SiH, BF₃-OEt₂, DCM; (iv) Boc₂O, TEA, DCM; (v) Pd/C, 1 atm H₂, EtOAc; (b) (i) NaBH₄/CoCl₂, EtOH; (ii) TFAA, TEA, DCM; (c) (i) I₂, HIO₃, MeOH/H₂O, reflux; (ii) LiOH-H₂O, MeOH/H₂O; (d) Pd(PPh₃)₄, TEA, 1 atm CO, THF, 60 °C; (e) (i) HCl/dioxane; (ii) **26**, TEA, EtOH, 60 °C.



Scheme 4. Reagents and conditions: (a) (i) NH₄BF₄, NaNO₂, HOAc/H₂O, concd HCl, 0 °C to rt; (ii) KOAc, EtOAc; (b) (i) AlCl₃, AcCl, DCE, 60 °C; (ii) Boc-3-piperidone, pyrrolidine, MeOH, 50 °C; (c) (i) NaBH₄, MeOH; (ii) Et₃SiH, BF₃-OEt₂, DCM; then HCl/dioxane; (iii) **26**, TEA, EtOH, 60 °C.

Table 3
Potency and selectivity of phenol replacement analogs

Compd	Akt1 IC ₅₀ ^a (μM)	PKA IC ₅₀ ^a (μM)	PKA/Akt1	pPRAS40 IC ₅₀ ^b (μM)
27	0.18	>10	>55	4.38
29	0.17	8.99	54	2.58
30	0.026	>10	>385	2.36
35	0.010	0.053	5	0.035
38	0.009	0.030	3	0.044

^a Data is an average of three determinations.

^b Data is an average of two determinations.

oxygen distance is 2.8 Å, while the indazole N to Ala230 NH is 2.9 Å. From an X-ray co-crystal of **38** bound to PKA (2.9 Å resolution), the distances are similar (indazole NH to Glu228 carbonyl oxygen 3.2 Å, indazole N to Ala230 NH 3.1 Å; structure not shown). Consequently, we hypothesize that the improved

hinge interactions observed for indazole **38** greatly benefit PKA inhibition while having modest effects on Akt potency, and thus PKA selectivity erodes for **38**. Note also that while amide **30** and lactam **35** have comparable Akt1 potencies, their PKA potencies are vastly different, suggesting that conformational constraint and the precise location of the hydrogen bond donor greatly influences PKA binding while not affecting Akt1. Taken together, these data reinforce the notion that interactions in the hinge region are particularly sensitive for PKA inhibition and that this phenomenon could be exploited to find selective compounds.

In summary, a novel series of spirochromane Akt inhibitors was discovered via HTS. Early SAR with a phenol hinge binder showed that optimization of the sulfonamide and amine side chain regions, as well as removal of the ketone from the spirochromane core, improved Akt1 enzyme potency and retained >250-fold selectivity over PKA. Further exploration of phenol replacements, such as a lactam and an indazole, produced compounds with much improved cell potency, but the PKA selectivity diminished to 5-fold. Select analogs were also examined for in vitro metabolism studies, and most showed very poor microsomal stability across species, which precluded further progression of these compounds (data not shown). Efforts to find a new chemical series that combines favorable Akt cell potency with high PKA selectivity will be reported in a forthcoming publication.

Acknowledgements

The authors would like to thank James M. Graham and Dr. Francis Sullivan for helpful discussions and careful proofreading in the preparation of this Letter.

References and notes

- (a) Hanks, S.; Hunter, T. *FASEB J.* **1995**, *9*, 576; (b) Zinda, M. J.; Johnson, M. A.; Paul, J. D.; Horn, C.; Konicek, B. W.; Lu, Z. H.; Sandusky, G.; Thomas, J. E.; Neubauer, B. L.; Lai, M. T.; Graff, J. R. *Clin. Cancer Res.* **2001**, *7*, 2475; (c) Masure, S.; Haefner, B.; Wesselink, J. J.; Hoefnagel, E.; Mortier, E.; Verhasselt, P.; Tuytelaars, A.; Gordon, R.; Richardson, A. *Eur. J. Biochem.* **1999**, *265*, 353.
- For recent reviews, see: (a) Wickenden, J. A.; Watson, C. J. *Breast Cancer Res.* **2010**, *12*, 202; (b) Bowles, T. L.; Parsons, C.; Muilenburg, D. J.; Bold, R. J. *Curr. Cancer Ther. Rev.* **2009**, *5*, 288; (c) Sarker, D.; Reid, A. H. M.; Yap, T. A.; de Bono, J. S. *Clin. Cancer Res.* **2009**, *15*, 4799; (d) Franke, T. F. *Oncogene* **2008**, *27*, 6473; (e) *Oncogene* **2008**, *27*, 5511; (f) Steelman, L. S.; Stadelman, K. M.; Chappell, W. H.; Horn, S.; Bäsecke, J.; Cervello, M.; Nicoletti, F.; Libra, M.; Stivala, F.; Martelli, A. M.; McCubrey, J. A. *Expert Opin. Ther. Targets* **2008**, *12*, 1139; (g) Manning, B. D.; Cantley, L. C. *Cell* **2007**, *129*, 1261.
- (a) Lindsley, C. W. *Curr. Top. Med. Chem.* **2010**, *10*, 458; (b) Lindsley, C. W.; Barnett, S. F.; Layton, M. E.; Bilodeau, M. T. *Curr. Cancer Drug Targets* **2008**, *8*, 7; (c) Lindsley, C. W.; Barnett, S. F.; Yaroschak, M.; Bilodeau, M. T.; Layton, M. E. *Curr. Top. Med. Chem.* **2007**, *7*, 1349. and references cited therein.
- Compounds **1** and **2** are mixtures of four stereoisomers.
- (a) Blake, J. F.; Kallan, N. C.; Xiao, D.; Xu, R.; Bencsik, J. R.; Skelton, N. J.; Spencer, K. L.; Mitchell, I. S.; Woessner, R. D.; Gloor, S. L.; Risom, T.; Gross, S. D.; Martinson, M.; Morales, T. H.; Vigers, G. P. A.; Brandhuber, B. J. *Bioorg. Med. Chem. Lett.* **2010**, *20*, 5607; (b) Bencsik, J. R.; Xiao, D.; Blake, J. F.; Kallan, N. C.; Mitchell, I. S.; Spencer, K. L.; Xu, R.; Gloor, S. L.; Martinson, M.; Risom, T.; Woessner, R. D.; Dizon, F.; Wu, W.; Vigers, G. P. A.; Brandhuber, B. J.; Skelton, N. J.; Prior, W. W.; Murray, L. J. *Bioorg. Med. Chem. Lett.* **2010**, *20*, 7037.
- For all of the analogs described herein, the Akt2 and Akt3 potencies followed similar trends to Akt1 potency, albeit with activities ca. 5- to 10-fold less potent.
- Potencies in the Akt1 enzyme assay as well as the phosphorylation of PRAS40 in LNCaP cells were measured as described in Ref. 5a.
- The relative configurations at the spiro piperidine stereocenters of **7-d1** and **7-d2** were not determined.
- Generated as outlined in Scheme 1 using ethoxyethylamine, 2,6-dimethylphenylsulfonyl chloride, and (*R*)-epichlorohydrin.
- An inseparable mixture of the Boc-deprotected styrene and fully reduced core were formed during step (a) (iii) in Scheme 3. Thus, Boc reprotection and hydrogenation were required to provide spirochromane intermediate **31** cleanly.